SEA SPRAY ICING PROFILES ON FIXED OFFSHORE STRUCTURES

Kathleen F. Jones
Terrestrial and Cryospheric Sciences Branch, CRREL, Hanover, New Hampshire USA
kathleen.f.jones@usace.army.mil

***Abstract*:** While ships create spray by slamming into waves as they push through the wave field, spray impinging on fixed platforms comes primarily from drops generated from wind waves. I determine spray drop profiles over the ocean using a published concentration density function for drops created by bursting bubbles. That function has been extended to very high wind speeds to include drops created by the wind ripping water off the crests of waves. Above the water, in the atmospheric surface layer, the spray concentration profile is assumed to follow a power law, based on friction velocity and drop fall velocities. I use drop concentration profiles based on measured meteorological data to determine the vertical profile of liquid water content, median volume radius, and spray icing rate on components of fixed offshore platforms. I compare simulated icing rates with semi-quantitative icing observations in very high winds on the semisubmersible exploration and drilling platform Ocean Bounty.

I. INTRODUCTION

Sea spray drops are carried by the wind and impact objects in their path. When the air temperature is below 0°C, spray drops may accrete as ice on ships and offshore structures. Many offshore structures, including semisubmersible oil exploration and production platforms, are fixed and have little area at the waterline. For those structures, sea spray impacting the superstructure comes from wind waves.

In this paper I extend the analysis in [1], focusing on the variation with elevation of liquid water content and median volume drop radius. Using weather and wave data from a semisubmersible offshore platform in Cook Inlet, Alaska, I simulate sea spray icing on cylindrical components at various elevations on the platform. Estimates of the variation in icing rate with elevation and cylinder diameter are obtained using the calculated collision efficiency and an ice density formulation. The resulting ice accumulation rates are compared to the semi-quantitative observations of the icing rates on the platform.

2. SEA SPRAY CONCENTRATION PROFILES

The sea spray concentration density function $\mathrm{d}C(r)/\mathrm{d}r$, the number of drops per cubic meter per micron

$$\frac{\mathrm{d}C(r)}{\mathrm{d}r} = \frac{7\mathrm{x}10^4 U_{10}^{\;2}}{r} \exp\left(-\frac{1}{2}\left[\frac{\ln(r/0.3)}{\ln 2.8}\right]^2\right) \tag{1}$$

applies for U_{10}, the wind speed at 10m, between 5 and 20 m s^{-1} [2]. It represents film and jet drops, which are created when the bubbles in whitecaps burst. As wind speed increases, the wind begins to rip the tops off of waves, creating spume drops, which tend to be larger than film and jet drops. Reference [2] revises (1) to include spume generated at high wind speeds. That spray concentration density function has a stronger dependence on wind speed and a longer tail:

$$\frac{\mathrm{d}C(r)}{\mathrm{d}r} = \frac{30U_{10}^{\;4}}{r} \exp\left(-\frac{1}{2}\left[\frac{\ln(r/0.3)}{\ln 4}\right]^2\right). \tag{2}$$

The spray drops are created at the ocean surface and carried aloft by turbulent convection. Small drops, with smaller gravitational settling velocities v_g tend to remain aloft longer than large drops. The drop concentration at elevation z is given by [3]:

$$\frac{dC(r,z)}{dr} = \frac{dC(r,h)}{dr}\left(\frac{z}{h}\right)^{-\frac{v_g}{\kappa u*}}, \tag{3}$$

with Kármán constant κ=0.4 and friction velocity $u*$. Height h is the upper limit of the source region for spray drop production. The sea spray liquid water content density function W(r,z) is determined from the drop concentration density function.

I simulate total liquid water content W(z) and median volume drop radius r_{MVR}(z) based on meteorological and wave height measurements from the Ocean Bounty platform at the end of 1979 and plot profiles of these parameters as a function of time. Compared to typical values in supercooled clouds at the summit of Mt. Washington, where W = 0.1 to 1 g m^{-3} and r_{MVR} = 5 to 30 µm [5], sea spray liquid water contents are typically much smaller and median volume radii are larger.

3. REFERENCES

[1] Jones KF, Andreas EL. Unpublished. Sea spray concentrations and the icing of fixed offshore structures, submitted to *Quarterly Journal of the Royal Meteorological Society*.

[2] Lewis ER, Schwartz SE. 2004. Sea salt aerosol production: Mechanisms, methods, measurements, and models—a critical review. Geophysical Monograph 152, AGU: Washington, DC, USA, pp 17, 174.

[3] Fairall CW, Banner ML, Peirson WL, Asher W, Morison RP. 2009. Investigation of the physical scaling of sea spray spume droplet production. *Journal of Geophysical Research* 114, C10001. DOI: 10.1029/2008JC004918.

Sea spray icing profiles on fixed offshore structures

Kathleen F. Jones
Terrestrial and Cryospheric Sciences Branch
Cold Regions Research and Engineering Laboratory
Hanover, New Hampshire USA
kathleen.f.jones@usace.army.mil

***Abstract*--While ships create spray by slamming into waves as they push through the wave field, spray impinging on fixed platforms comes primarily from drops generated from wind waves. I determine spray drop profiles over the ocean using a published concentration density function for drops created by bursting bubbles. That function has been extended to very high wind speeds to include drops created by the wind ripping water off the crests of waves. Above the water, in the atmospheric surface layer, the spray concentration profile is assumed to follow a power law, based on friction velocity and drop fall velocities. I use drop concentration profiles based on measured meteorological data to determine the vertical profile of liquid water content, median volume radius, and spray icing rate on components of fixed offshore platforms. I compare simulated icing rates with semi-quantitative icing observations in very high winds on the semisubmersible exploration and drilling platform Ocean Bounty.**

Keywords-sea spray, offshore structures, icing profile

II. Introduction

Sea spray drops are carried by the wind and impact objects in their path. When the air temperature is below 0°C, spray drops may accrete as ice on ships and offshore structures. On ships, spray impacting the superstructure is created primarily by the vessel slamming into waves and swell as it powers through the water. However, many offshore structures, including semisubmersible oil exploration and production platforms, are fixed and have little area at the waterline. For those structures, sea spray impacting the superstructure comes from wind waves.

In this paper I extend the analysis in [1], focusing on the variation with elevation of liquid water content and median volume drop radius. Using weather and wave data from a semisubmersible offshore platform in Cook Inlet, Alaska, I simulate sea spray icing on cylindrical components at various elevations on the platform. Estimates of the variation in icing rate with elevation and cylinder diameter are obtained using the calculated collision efficiency and an ice density formulation. The resulting ice accumulation rates are compared to the semi-quantitative observations of the icing rate on the platform. I discuss possible explanations for the differences between simulation and observation and propose exploiting offshore platforms in northern seas to better quantify the processes controlling sea spray generation.

III. Sea Spray Concentration

Reference [2] provides a sea spray concentration density function, which can be rewritten in terms of d$C(r)$/dr, the number of drops with radius r per cubic meter per micron:

$$\frac{\mathrm{d}\,C(r)}{\mathrm{d}\,r}=\frac{7\text{x}10^4 U_{10}{}^2}{r}\exp\left(-\frac{1}{2}\left[\frac{\ln\left(r/0.3\right)}{\ln 2.8}\right]^2\right)\,. \qquad (1)$$

This function applies for U_{10}, the wind speed at 10m, between 5 and 20 m s^{-1}. It represents film and jet drops, which are created when the bubbles in whitecaps burst. As the wind speed increases, the wind begins to rip the tops off of waves, creating spume drops, which tend to be larger than film and jet drops. Reference [1] revises (1) to include spume generated at high wind speeds, using data from concentrations measured for U_{10} as high as 28.8 m s^{-1}. That spray concentration density function has a stronger dependence on wind speed and a longer tail:

$$\frac{\mathrm{d}\,C(r)}{\mathrm{d}\,r}=\frac{30 U_{10}{}^4}{r}\exp\left(-\frac{1}{2}\left[\frac{\ln\left(r/0.3\right)}{\ln 4}\right]^2\right)\,. \qquad (2)$$

These two functions are plotted in Fig. 1 for U_{10}= 6, 12, and 24 m s^{-1}.

The spray drops are created at the ocean surface and carried aloft by turbulent convection. Small drops, with smaller gravitational settling velocities v_g tend to remain aloft longer than large drops. Drops with radii of 12, 30, 240, and 500 µm have v_g of 0.02, 0.1, 2, and 4 m s^{-1}, respectively. The drop concentration at elevation z is given by [3]:

$$\frac{dC(r,z)}{dr}=\frac{dC(r,h)}{dr}\left(\frac{z}{h}\right)^{-\frac{v_g}{\kappa u^*}}, \qquad (3)$$

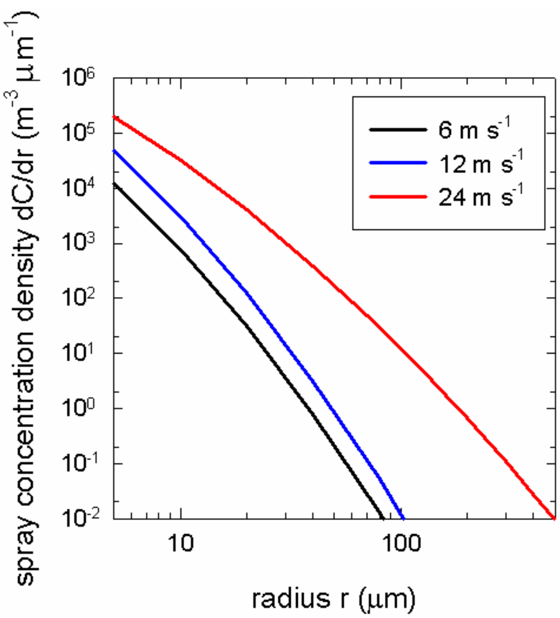

with Kármán constant κ=0.4 and friction velocity u^*. Height h is the upper limit of the source region for spray drop production. Film and jet drops are produced in

Figure 1. Sea spray drop concentration density functions: film and jet drops at 6 and 12 m s^{-1}; film, jet and spume drops at 24 m s^{-1}.

whitecaps, generally in the wave troughs on the windward side of the crest [4], so I use a nominal h =1 m for determining the profile for the source concentration given by (1).Spume drops are generated at the wave crest, so the profile resulting from the source concentration (2) has $h = 0.5H_{1/3}$, where $H_{1/3}$ is the significant wave height.

The sea spray liquid water content density function is determined from the drop concentration density function:

$$\frac{\mathrm{d}W(r,z)}{\mathrm{d}r} = \rho_w \frac{4}{3}\pi r^3 \frac{\mathrm{d}C(r,z)}{\mathrm{d}r}. \qquad (4)$$

The total liquid water content W(z) is the integral of (4) over radius. The median volume radius r_{MVR} of the drops is a useful characterization of sea spray. It is the drop radius for which half the water in the spray is in smaller drops and half is in larger drops. Simulated W(z) and r_{MVR}(z) based on meteorological and wave height measurements from the Ocean Bounty platform at the end of 1979 are shown in Fig. 2. Note the strong variation with wind speed and the weaker variation with elevation. Compared to typical values in supercooled clouds at the summit of Mt. Washington, where W = 0.1 to 1 g m^{-3} and r_{MVR} = 5 to 30 µm [5], sea spray liquid water contents tend to be much smaller and median volume radii are larger.

IV. ICE ACCRETION FORMULATION

The spray drops quickly cool to below the air temperature, so if $T(z) < 0^{o}$C the drops freeze to any structure they impact in flight. The flux of spray water is the product of dW(r,z)/dr and the wind speed U(z). The mass accretion rate per unit area dm(z)/dt on a cylinder with diameter D, with its axis perpendicular to the wind direction, is determined by the flux of spray drops and the collision efficiency E(U,r,D) [6] of the drops with the cylinder:

$$\frac{\mathrm{d}m(z)}{\mathrm{d}t} = U(z)\int_{r_{\min}}^{r_{\max}} E(U,r,D)\frac{\mathrm{d}W(r,z)}{\mathrm{d}r}\mathrm{d}r\,. \qquad (5)$$

The minimum drop radius $r_{\min}$=5 µm is reasonable, because the small drops have low collision efficiencies. Large drops are rare and have relatively large settling velocities, so $r_{\max}$=400 µm, is sufficiently large. The accretion of ice is often described in terms of its thickness rather than its mass. If I make additional assumptions about the shape and density of the ice that accretes, I can estimate the rate of change of the ice thickness. As shown in Fig. 2, sea spray liquid water contents are small so the drops are likely to freeze individually on impact, rather than coalescing and flowing around the cylinder before freezing. Therefore, I assume that the ice accretion cross-sectional shape is a semi-ellipse on the windward side of the cylinder with a semi-minor axis D/2, perpendicular to the wind direction, and a semi-major axis I+D/2. Then the icing rate in terms of thickness I is

$$\frac{\mathrm{d}I(z)}{\mathrm{d}t} = \frac{4}{\pi\rho_i}\frac{\mathrm{d}m(z)}{\mathrm{d}t}\,, \qquad (6)$$

where ρ_i is the density of the accreted ice.

Reference [7] reports densities of samples of spray ice taken from locations on the foredeck of a Coast Guard cutter during a cruise in the Bering Sea in February and March 1990. The sample densities range from 0.69 to 0.92 g cm^{-3} for ice that accreted at air temperatures ranging from 0 to -15°C. The spray that caused these ice accretions was generated by the ship slamming into waves. Reference [8] reports the characteristics of this ship-generated spray. The liquid water contents ranged between 1.1 and 1163 g m^{-3}, with a median value of 64 g m^{-3}. The median volume radii ranged between 85 and 3050 µm, with a median value of 550 µm. In comparison, for U_{10} up to 39.5 m/s, the simulated sea spray liquid water content ranges up to 0.082 µm and median volume radius ranges from 11 to 94 µm (Fig. 2).

The characteristics of sea spray generated from wind waves are more similar to the characteristics of clouds than they are to the characteristics of ship-generated spray. Therefore, I use a rime density relationship determined from multicylinder data at Mt. Washington [9] as a first attempt to estimate accreted ice densities from sea spray on fixed offshore platforms:

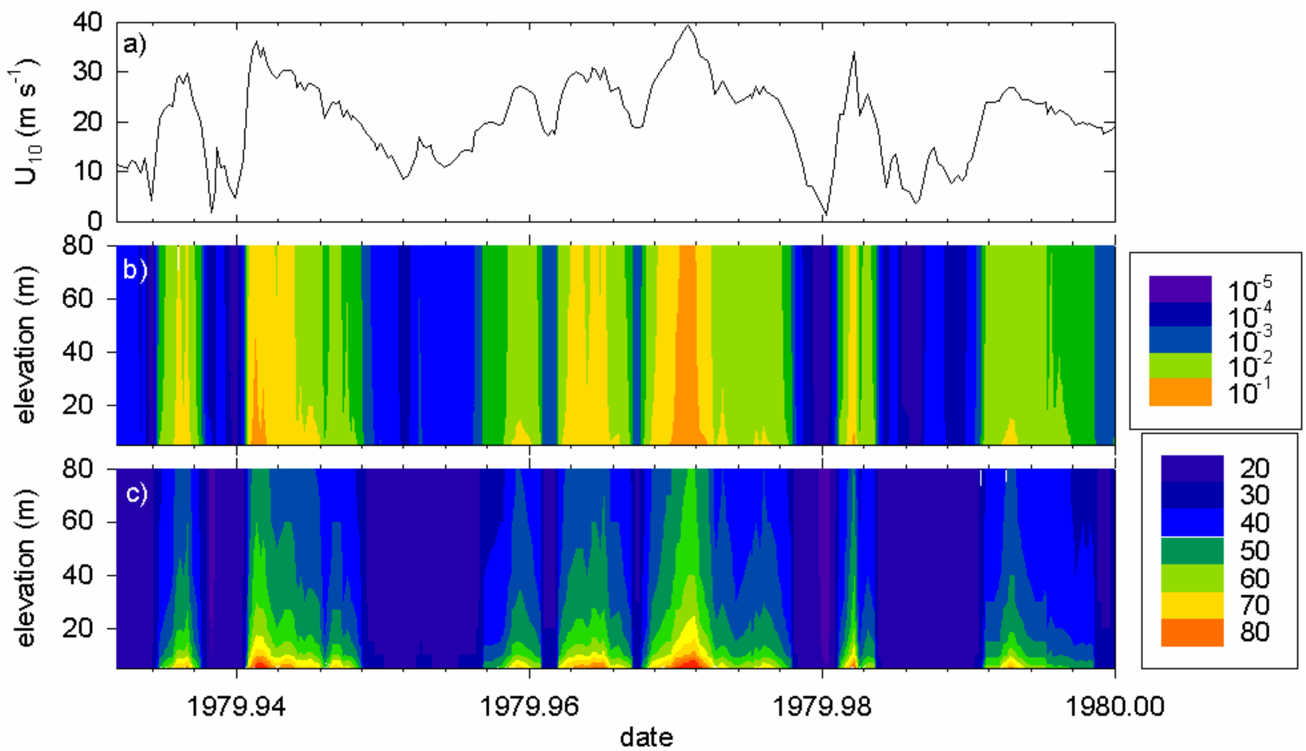

Figure 2. a) Wind speed at 10 m on the semisubmersible Ocean Bounty for the last 3 weeks and 3 days of 1979, b) simulated sea spray liquid water content, and (c) simulated median volume drop radius.

$$\rho_i = 1.335 + 0.1010\log\left(\frac{EW}{\rho}10^{-6}\right) + 0.4137E$$
$$+2.437\frac{k_a T_a}{\mu_a L_f} + 38.29\frac{V^2}{L_f}10^{-3} \quad , \qquad (7)$$

where ρ_i is in units of g cm^{-3}, μ_a [g cm^{-1} s^{-1}] =0.000171 +5.2x10^{-7}T_a is the dynamic viscosity of air at temperature T_a, k_a [J cm^{-1} s^{-1} ^{o}C^{-1}] = 4.186x10^{-7}(573 + 1.8T_a) is the thermal conductivity of air, and L_f=334 J g^{-1} is the latent heat of fusion of water. Convenient units are used in (7), with the powers of ten in the second and last terms for the conversion to consistent units. Equation (7) does not account for the salinity of the spray drops and the brine that is ejected as the drops freeze. I expect it to provide only a rough estimate of the spray ice density. If the computed density from this equation is unrealistically high or low in spray ice accretion simulations, it is constrained to minimum and maximum values of 0.1 and 0.9 g cm^{-3}, respectively.

V. Ocean Bounty spray icing events

Spray icing of the semi-submersible exploratory drilling rig Ocean Bounty during the winter of 1979-1980 is described in [10], [11], [12], and [13]. The Ocean Bounty is 107 m long and 81 m wide, with the main deck 16 m above the ocean surface. The anemometer was 84 m above sea level. The rig was operated by Phillips Petroleum Company near Kamishak Bay in Lower Cook Inlet, Alaska, 20 km from shore in 160 m of water.

From 24 September 1979 to 26 April 1980 meteorological and oceanographic data were recorded by Oceanroutes, Inc., meteorologist-observers every day. Beginning 20 December 1979, superstructure icing was added to the daily data sheets and was recorded as light, moderate, heavy, or very heavy, following [13], which quantifies icing rates in inches per day as 0.04 to 1.4 (light), 1.4 to 2.6 (moderate), 2.6 to 5.7 (heavy), and 5.7+ (very heavy). Note that inches day^{-1} is essentially the same as mm hr^{-1}. There is no information about where on the Ocean Bounty the icing rate observations were made. Weather, sea, and icing parameters were recorded every two hours from 0600 to 1800 LST. Some of those parameters were also recorded at 0200 and 2200. Water temperature was measured once a day at 1400. Scanned copies of the data sheets were provided to me by the Department of the Interior's Minerals Management Service (now Bureau of Ocean Energy Management, Regulation and Enforcement).

Fig. 3 shows (a) the air temperature T_a (assumed to be measured at 84 m also) and water temperature T_s, (b) U_{10} calculated from the measured wind speed, and (c) observed $H_{1/3}$. The threshold wind speed for the

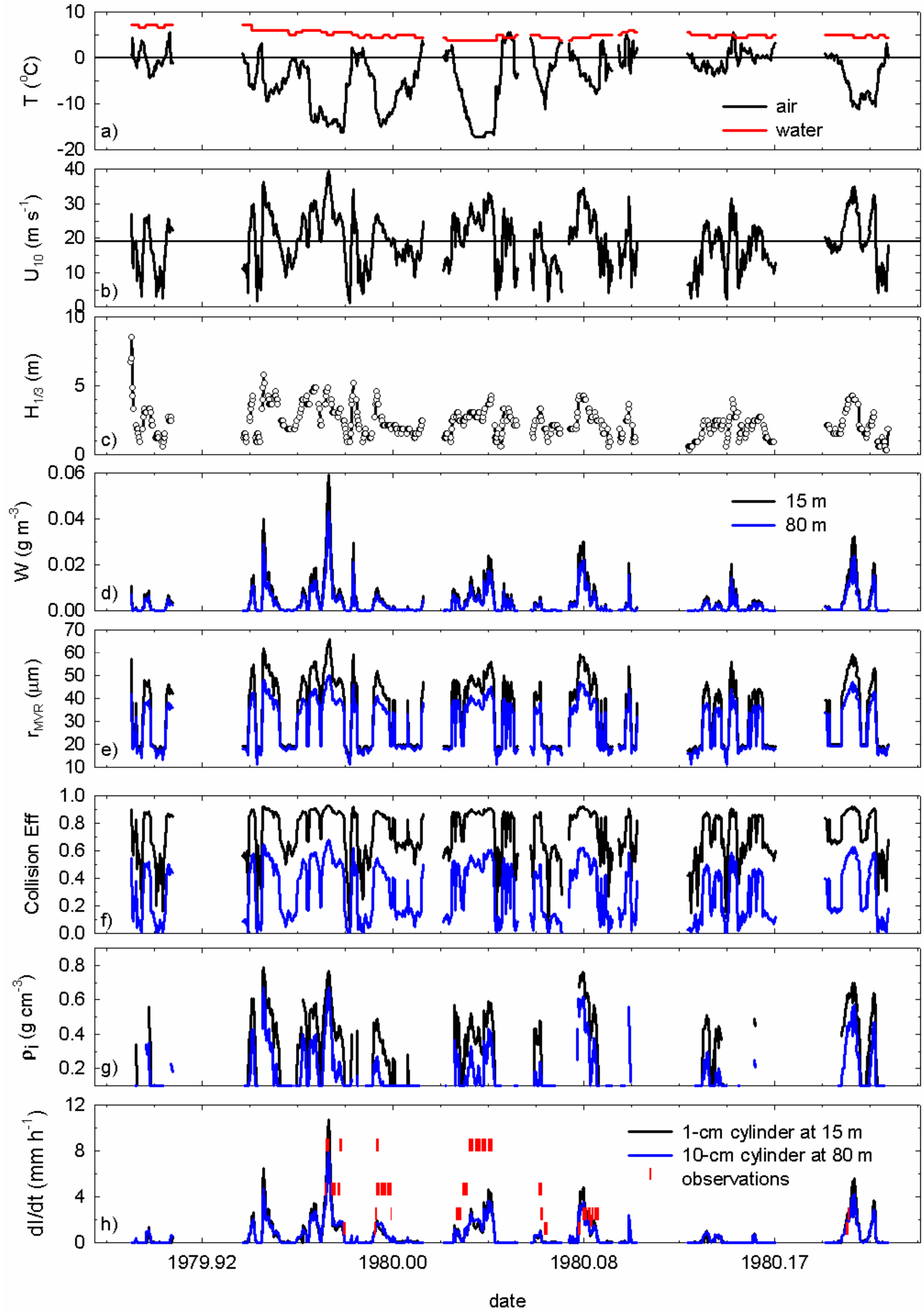

Figure 3. Ocean Bounty observations and simulations, winter of 1979-1980 a) air temperature, b) wind speed at 10 m, c) significant wave height, d) sea spray liquid water content, e) sea spray median volume drop radius, f) average collision efficiency, g) density of accreted ice, h) icing rate.

generation of spume drops is shown as a line at 19 m s^{-1}. For lower wind speeds I use (1) to determine the drop concentration density, and for higher wind speeds I use (2). Major tick marks on the horizontal axis indicate 1/12 of a year (~ 1 month), with minor ticks indicating 1/4 of a month (~ 1 week). The data underlying these plots is available in electronic format on request.

I calculate the spray liquid water content and median volume drop radius using (1) through (4) and plot them at elevations of 15 m and 80 m in Fig. 4d and e, respectively, to illustrate their variation from the level of the main deck up to the anemometer. Larger drops fall out of the spray at lower elevations than smaller drops, which also causes a decrease in liquid water content as elevation increases. The smaller r_{MVR}s aloft lead to lower collision efficiencies aloft. The overall collision efficiencies for a 1-cm-diameter cylinder at 15 m and a 10-cm diameter cylinder at 80 m are shown in Fig. 4f. The last two panels show results from modeling the accretion of ice from the sea spray for these two cases. For hours with T_a<0°C, estimated ice density (7) is shown in Fig. 4g. In most conditions the calculated value is greater than the prescribed 0.1 g cm^{-3} minimum and less than the spray ice densities reported for ships, thus passing the sanity test. The simulated icing rates calculated using (5) and (6) are in Fig. 4h, along with the observations of icing rate from the daily data sheets. Recall that the icing rate observation was added to the daily data sheet on 20 December, apparently following the first spray icing event in early December. In three of the six storms with recorded icing rate observations, the observed rates are significantly greater than the simulated rates.

VI. Discussion

The reasons for the varying level of agreement between the observed icing rate and the simulated rate in Fig. 4h are not obvious.

The simulation focused on two disparate situations: a 1-cm-diameter cylinder at 15 m above the ocean surface, and a 10-cm-diameter cylinder at 80 m. The first case has larger liquid water contents, median volume drop radii, and collision efficiencies than the second case, and therefore higher accreted ice densities. The simulation shows that the smaller mass and the lower density of accreted ice aloft results in an icing rate, in terms of thickness, that is nearly the same as that on the 1-cm cylinder at 15 m. Thus, for the comparison between observations and simulations, knowing the specifics of the icing observations does not appear to be important.

A possible explanation for the difference between simulation and observation is that the fourth power of U_{10} in (2) is too big. A smaller power for U_{10} with a commensurate increase in the multiplier would result in a less pronounced increase in concentration with wind speed. The effect of such a change on Fig. 4h would be to decrease the differences between the simulated icing rates in the six observed icing events.

By taking advantage of drilling and exploration platforms in northern oceans, researchers have the opportunity to contribute to understanding and quantifying sea spray associated with wind waves. Simultaneous multicylinder observations [15] at a number of elevations on such a platform, supplemented by weather and sea state observations, would characterize the variation of liquid water content and median volume drop radius of the spray. This research would also allow us to reliably forecast icing on fixed offshore platforms, as is currently done for ships [16].

Acknowledgment

This work was supported by U.S. Department of the Interior Minerals Management Service (MMS) under Interagency Agreement M07RG13274.

References

[4] Jones KF, Andreas EL. Unpublished. Sea spray concentrations and the icing of fixed offshore structures, submitted to *Quarterly Journal of the Royal Meteorological Society*.

[5] Lewis ER, Schwartz SE. 2004. *Sea salt aerosol production: Mechanisms, methods, measurements, and models—a critical review*. Geophysical Monograph 152, AGU: Washington, DC, USA, pp 17, 174.

[6] Fairall CW, Banner ML, Peirson WL, Asher W, Morison RP. 2009. Investigation of the physical scaling of sea spray spume droplet production. *Journal of Geophysical Research* 114, C10001. DOI: 10.1029/2008JC004918.

[7] de Leeuw G. 1990. Profiling of aerosol concentrations, particle size distributions and relative humidity in the atmospheric surface layer over the North Sea. *Tellus* 42B: 342–354.

[8] Jones, KF. 1990. The density of natural ice accretions related to nondimensional icing parameters. *Q.J. Royal Meteorological Society* 116: 477-496.

[9] Finstad KF, Lozowski EP, Gates EM. 1988. A computational investigation of water droplet trajectories. *Journal of Atmospheric and Oceanic Technology* 5: 160–170.

[10] Ryerson CC, Gow AJ. 2000. '*Ship superstructure icing: crystalline and physical properties*', ERDC/CRREL Technical Report TR-00-11, 35pp. Cold Regions Research and Engineering Laboratory: Hanover, New Hampshire, USA.

[11] Ryerson CC 1995. Superstructure spray and ice accretion on a large U.S. Coast Guard cutter. *Atmospheric Research* 36: 321-337.

[12] Thorkildson RM, Jones KF, Emery MK. 2009. In-cloud icing in the Columbia Basin. *Monthly Weather Review* 137: 4369-4381.

[13] Williams JA. 1981. 'Charting heavy Alaskan weather'. *Offshore* 5 June 1981. pp 49–54. PennWell Petroleum Group: Houston, Texas, USA.

[14] Nauman JW. 1984. 'Superstructure icing on the semi-submersible Ocean Bounty in Lower Cook Inlet, Alaska'. In *Proceedings of the 2nd International Workshop on Atmospheric Icing of Structures, EFI Technical Report 3439*, pp 71–79, Trondheim, Norway 19-21 June 1984.

[15] Minsk LD. 1984. '*Assessment of ice accretion on offshore structures*', CRREL Special Report 84-4, 12pp, Cold Regions Research and Engineering Laboratory, Hanover, New Hampshire, USA.

[16] Nauman JW, Tyagi R. 1985. 'Sea spray icing and freezing conditions on offshore oil rigs—Alaska experience and regulatory implications'. In *Proceedings of the International Workshop on Offshore Winds and Icing*, pp 57–68, Halifax, Nova Scotia, 7–11

October 2005. Atmospheric Environment Service, Downsview, Ontario, Canada.

[17] Wise JL, Comiskey AL. 1980. '*Superstructure icing in Alaskan waters*', NOAA Special Report, 30pp. Contribution No. 468 from NOAA/ERL. Pacific Marine Environmental Laboratory: Seattle, Washington, USA.

[18] Howe J. 1991. Rotating multicylinder method for the measurement of cloud liquid water content and droplet size. CRREL Report 91-2, 18 p.

[19] Overland, J E, Pease CH, Preisendorfer RW, and Comiskey AL. 1986. Prediction of vessel icing. ***J. Climate Appl. Meteor.*** 25:1793–1806.